OPTICAL PRESCRIPTION OF THE HST

David Redding, Sam Sirlin, Andy Boden
Jet Propulsion Laboratory, California Institute of Technology
Jinger Mo, Bob Hanisch
Space Telescope Science Institute
Laurie Furey
Optical Archeology, Inc.

July 25,1995

Abstract. The optical prescription of the Hubble Space Telescope is estimated by prescription retrieval from defocused WF/PC-II images. New formulas relating the 11ST primary mirror conic constant and spherical aberration are presented. These new formulas reconci le long-standing differences between estimates of the conic constant derived from phase retrieval and estimates derived by other means.

1. Introduction

The optical prescription of the Hubble Space Telescope - in particular the conic constant of the primary mirror - received a lot of attention following discovery of the spherical aberration of the primary mirror. The concern then was to design appropriate corrective optics for WF/PC-II and COSTAR. This concern remains today, though at a different level, for builders of future instruments, especially of instruments that might seek to compensate for primary mirror (PM) aberrations on a finer spatial scale (Malbet, 1995).

Under the Hubble Aberration Recovery Program (HARP), several groups independently determined estimates of the PM conic (Moore, 1991). Complete agreement among the groups was not achieved, Those who examined the fabrication and test hardware (the "fossil data" study) derived a number for the PM conic of -1.01377±0.0003 (Furey, 1993). Several more groups who employed phase retrieval techniques derived numbers ranging from -1.0137 to -1.0150 (e.g. Fienup, 1993; Roddier, 1993; Shao, 1991). The official estimate used to build COSTAR (-1.0139) averaged rt'suits from several studies, but did not resolve the differences. These differences were emphasized again recently, with publication of phase retrieval results from WF/PC-II data indicating a value for the primary mirror conic const ant of -1.0144 (Krist, 1995).

Also as part of the HARP effort, a direct prescription retrieval technique was developed and applied (Redding, 1993). Like phase retrieval, prescription retrieval is an "image inversion" parameter estimation approach, where a computer model of the optical system is used to generate simulated images that are matched iteratively with data images. The HART) prescription retrieval results agreed with the fossil data studies, with an estimate of -1 .01398+0 .0002.

Prescription retrieval differs from phase retrieval in the parametrization of the image-inversion problem. It uses a hybrid ray-trace and diffraction modeling code to solve *directly* for the conic constant and other prescription parameters. By contrast, phase retrieval techniques solve for intermediate wavefront phase para meters, usually Zernike polynomials. The effect of the conic constant error appears as spherical aberration, or the

11th Zernike polynomial coefficient ("211") in the 33%-obscured form used by HST investigators. in a crucial step, the conic constant is then estimated from Z11 using a simple formula derived using ray-trace techniques (1 'urey, 1991).

In this paper, we report new results using prescription retrieval to estimate the PM conic from WF/PC-II focus run images. These preliminary results agree with the HARP fossil data and prescription retrieval results, They disagree with reported estimates of PM conic derived from phase retrieval results using the old formula.

To resolve these differences, we reexamine the formula used to compute conic constant from 211. Using higher ray densities than was possible originally, and computing formulas for each camera separately, new formulas are derived. These formulas are used to reprocess the spherical aberration results reported by the phase retrieval studies. The resulting estimates of conic constant are in agreement with the earlier official estimate. Combining all results (reprocessed phase retrieval, fossil data and prescription retrieval), the primary mirror conic constant is estimated to be - 1.0139f0.0002.

The HST prescription is also of interest for image restoration purposes. We use prescription-based PSF generation codes to support spatially -variant-PSF image restoration (Redding, 1994; Boden, 1995). Prescription retrieval is used to obtain the accurate prescription data needed to generate representative PSFs.

2. Prescription Retrieval

The HST Optical Telescope Assembly (OTA) consists of a primary and a secondary mirror, plus supports and baffles, forming a Ritchey-Chretien telescope (Burrows, 1990) (Fig. 1). The WF/PC imaging camera optics follow the OTA optics, beginning with a pickoff mirror (POM) at the center of the OTA field of view (Burrows, 1995). Then comes the filter wheel and a pyramid mirror, which splits the field of view into 4 separate cameras. Within each camera there is a fold mirror followed by the WF / PC repeater optics. These consist of a repeater primary (RPM), secondary mirror (RSM), and CCD detector assembled together in a barrel structure. Field curvature is corrected by a plano-concave field flattener lens mounted immediately in front of the detector.

In WF/PC-II, the pupil is reimaged at the RSM, which is figured to compensate for the spherical aberration of the OTA primary. The WF/PC-II design was frozen before the HARP results were finalized, however. The best estimate of K at the time the RSM design was frozen was -1.0135, so this is the value that the compensation was designed to null. Later results showed the primary to be slightly more aberrated (K= -1 .0139). The result is that the WF/PC-II compensation leaves a small residual spherical aberration, which is seen in the data.

The precise footprint of the beam on the WF/PC-II RSM can be adjusted on-orbit by tilting the pick-off mirror and, in PC-1, WF-3 and WI -4, by tilting the camera fold mirrors. Errors in placing the beam on the RSM result in coma in the image.

Focus is adjusted by axial translation of the OTA secondary. The OTA secondary can also be recentered to recollimate the telescope. Small misalignments incurred in fabrication are to be expected in the repeater barrel position and angle, plus all individual optics.

Obscurations affecting the image are incurred at the OTA secondary support spiders and baffles, and at the OTA primary, where 3 small support pads are visible at the edges of the aperture. The entrance aperture is placed about 88 mm ahead of the primary mirror, defining the system stop. There is field-angle dependent vignetting at the filters and at the RSM. The location in the pupil of the RSM obscurations is also strongly dependent on field angle. The amount of light passed by the HST and WF/PC-II system varies by about 15% over the full WF field.

In addition to the shearing obscuration effects, there are induced aberrations and distortion that occur with changes in field angle. Small amounts of coma and astigmatism are seen at the edges of the field.

All of these systematic effects on the HST PSF can be accurately predicted from the optical prescription using a combination of ray-trace and physical optics techniques. Here "optical prescription" means the data defining the orientation, location, figure and index of each optical element. Prescription-based ray-trace codes can accurately determine the wavefront phase and obscuration patterns induced by changing field angles, changing focus or decenter of the secondary, or by misalignment of any of the other optics in the beam train. This is how optical systems are designed, after all.

Fourier optics diffraction beam propagators can then be used to convert ray-based phase information into aTE complex-amplitude matrix describing the diffracted beam. This can be done at multiple points in the beam train, if desired, though here it is sufficient to use a single diffraction propagation, from the exit pupil to the detector. The detected intensity is the modulus squared of the field at the detector, resampled into the CCD pixel resolution. Detection effects, such as charge-transfer blurring, motional blurring and noise can then be added.

This approach to modeling optical instruments is realized in a general-purpose optical modeling code called COMP (Redding, 1992). COM1' uses the optical prescription to define the image-forming beam train. It uses a full general ray-trace engine to trace a bundle of rays defined at entrance pupil past each optical, vignetting or obscuring surface. The exit-pupil phases computed by the ray-trace drive a Fourier beam propagator, which computes the diffracted image at the detector.

The COMP model provides means to capture the systematic behavior of the images, provided accurate prescription data is used. In general, the design prescription, or even a prescription incorporating results of ground testing will not capture the full performance of the instrument. Means to improve estimates of prescription parameters beyond pre-launch values are provided by prescription retrieval.

Prescription retrieval is an iterative parameter optimization process (Fig. 2), taking the optical design prescription as a starting point, generating images at particular field and focus settings, and matching these images to data images taken under the same conditions (Redding, 1993). The match is improved by varying selected prescription parameters. Some parameters vary with each image in a set, such as field angle, flux, background, and focus setting. Other parameters are common to a set of images, such as

OTA and WF/PC mirror figure parameters, OTA higher-order figure errors, WF/PC barrel alignments, and pickoff mirror and fold mirror tilts.

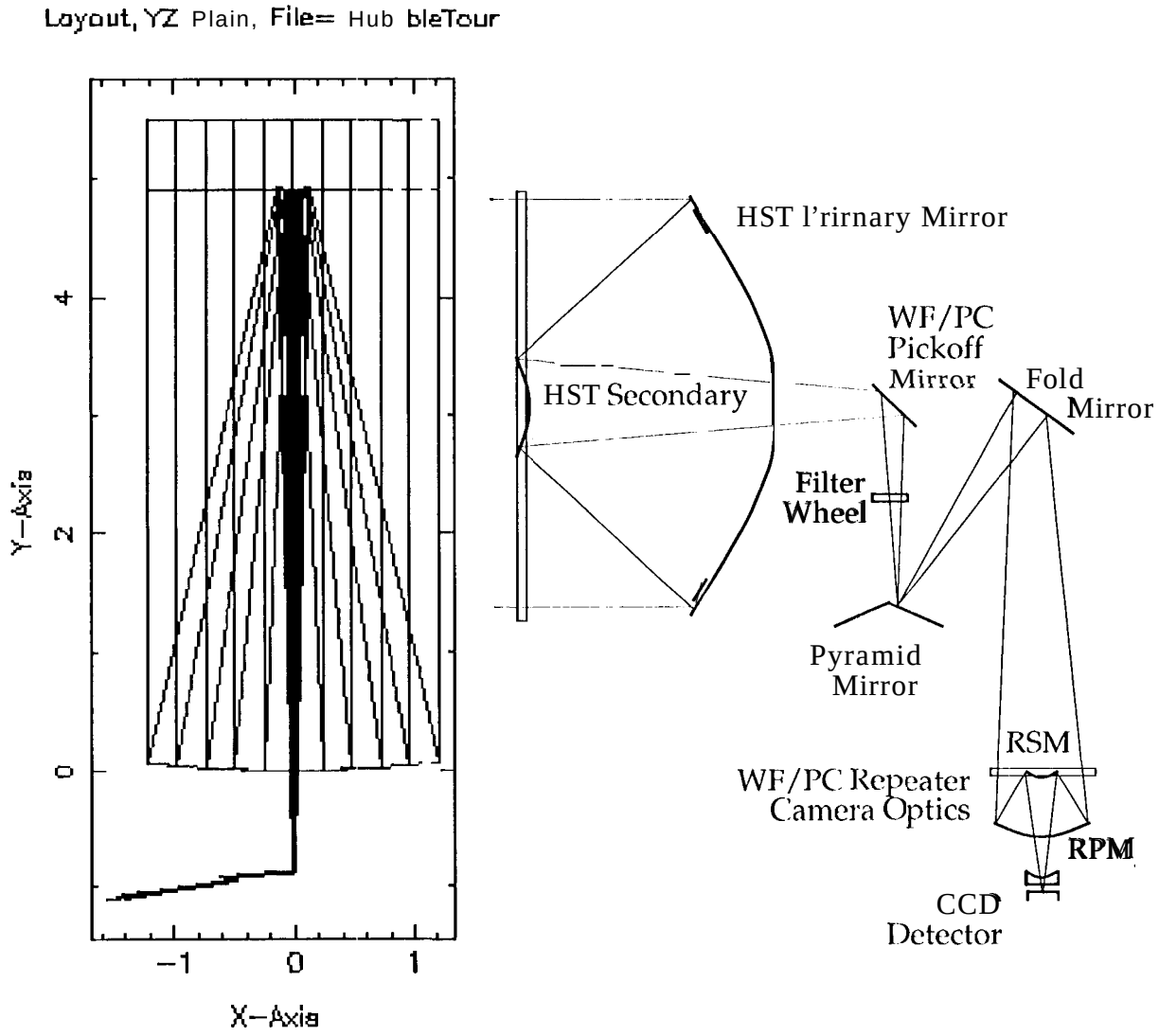

Figure 1. Ray-trace of the HST and WF/PC-I

To get good results for most parameters, a good set of diagnostic images is needed. This should include images taken at multiple focus positions, at multiple field points, and in multiple cameras. Defocusing spreads out the images across many pixels, exposing the signature of the aberrations, such as the spherical aberration rings, and improving the ability to resolve these features. Data taken from both sides of focus resolves ambiguities between asymmetric surface figure aberrations. Defocusing also brings out the obscuration patterns, which help identify alignments. Field diversity shears the effects induced at different surfaces. This was useful in WF/PC-I retrievals, as it separated the aberration centers of the OTA optics from the aberration centers of the repeater cameras: the OTA aberrations remain centered while the camera aberrations shift center with field

angle, improving the separability of these contributors to the overall HST spherical aberration.

I'description retrieval is a better approach than phase retrieval for determining the prescription of an instrument, because it directly solves for the parameters of interest in a model that accurately represents their effect on the data. On the other hand, phase retrieval can be very effective in matching particular images, Zernike polynomials provide a less-constrained, nearly orthonormal phase parameter set compared to prescription parameters. Non-parametric phase retrieval has the further advantage of a very large number of degrees of freedom for matching data.

The problems with phase retrieval have to do with converting the phase information to prescription information (this is discussed in detail later), and in extrapolating fits at one field / focus point to another. Generalizing a match at one point to predict the PSF at another using a conventional physical optics model requires separately identifying and fitting models to all of the systematic variations that occur with changes in field angle and focus. This includes shearing obscurations, shearing figure errors, and varying aberration and distortion terms. Prescription-based models provide a better basis for predicting these systematic effects.

Either approach can be carried too far, by overfitting the data at high spatial frequencies, so that effects such as scattered light and detection blurring can be incorrectly attributed to optical aberrations. The likelihood of this can be reduced by avoiding scattered or stray light conditions in the data, by including detection blurring in the model, and by using a sufficiently large and diverse data set.

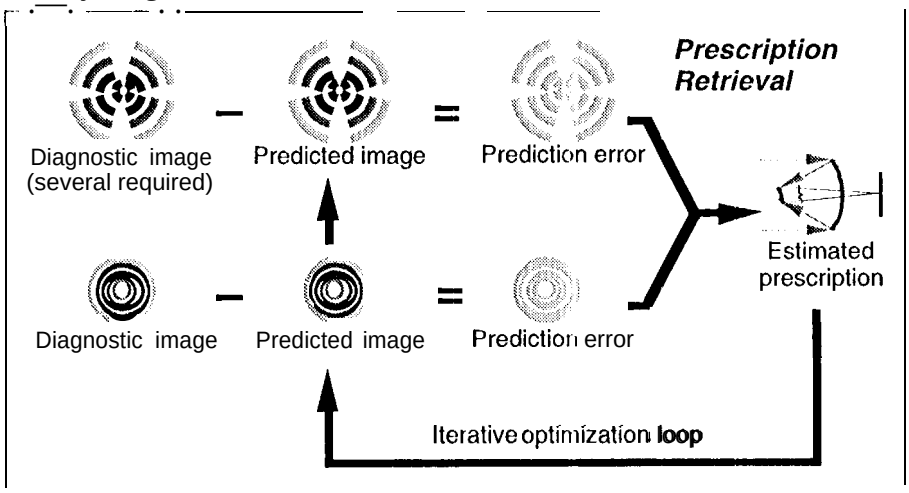

Figure 2. Sketch of prescription retrieval proms.

3. WF/PC-II Prescription Retrieval Preliminary Results

This section reports preliminary results of prescription retrieval using WF/PC-II images. Defocused data was taken by the WF/PC-II team soon after the servicing mission. These images were taken on-axis, at 4 focus settings (±360 urn and ±180 um defocus). They were taken in all 4 cameras, using 3 narrow-band filters. Two images were taken for each setting. Cosmic-ray and saturated pixel identification was performed to generate masks

for each image. Most results were run with combined images (the 2 images were added), though some were run with single images.

The objective of this first round of retrievals was to determine if the defocused images are consistent with previous estimates of the prescription parameters. The starting prescription was taken to be the WF/PC-II project official "as-bui It" Code V'[M] prescription. Image-specific parameters varied were field angle, flux, background, and focus setting. System parameters, assumed the same in each image, were the conic constants of the OTA primary and secondary, the conic constants of the repeater camera primary and secondary, WF/PC barrel alignments, and pickoff mirror and fold mirror tilts. In addition, 2 of the runs included Zernike figure errors on the primary mirror. No detection blurring was included in these retrievals.

The individual images were fit fairly well at lower spatial frequencies. The main features for determining the conic constants, namely the brig] ıt spherical aberration rings, appear at the same positions. Other features were not matched as well, and we expect that including higher spatial-frequency figure errors and detector blurring will improve the overall match. Figure 3 shows images from PC1 Run 2, comparing simulated and data images for OTA secondary mirror defocus = 360 urn. Figure 4 compares simulated and data images for defocus = 180 urn..

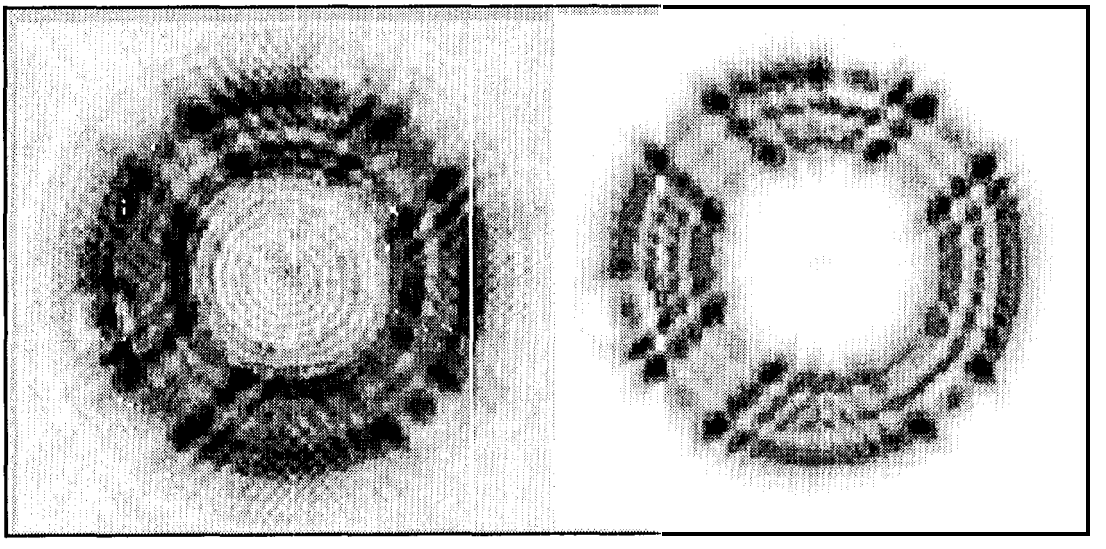

Figure 3. Data (left) and simulated (right) images from WF/PC-II, PC-1 camera (Run 2). Secondary mirror defocus=360 microns; Filter=F502N.

The results for mirror conic constants are summarized in Table 1. The initial parameter values for the first 4 runs were set to the "as built" official estimates. All conies were allowed to vary, together with other image and system parameters. The results show very little change in the estimates of the OTA conic constant parameters. The PC-1 repeater conic constant estimates also change very little. This is consistent with test results that show only a very small amount of spherical aberration in the PC-1 repeater camera (Krist, 1995). The estimates of the WF-2 repeater conies change more significantly; those for WF-3 change very little.

To test the hypothesis that the OTA PM conic is actually less than -1.0139, and to test the separability of the conic parameters, initial values for the last 2 cases were set at lower values (-1 .0141 and -1.0144, respectively). The estimates of the OTA PM conic did not converge to the same numbers. The overall spherical aberration remained about the same, however, as the increased spherical aberration from the I'M was reduced by changes in the estimated conies for the other cameras (the Z11 numbers were fit to OPD maps generated using the retrieved prescriptions). The indication is that this data does not provide sufficient diversity to separate the contributions of figure errors at multiple surfaces. This being the case, the most likely results are those which require the least change in the "as built" a priori estimates. Runs 1-4 are to be preferred on these grounds. The conclusion is that the data is consistent with the "as-built" estimates of the OTA prescription.

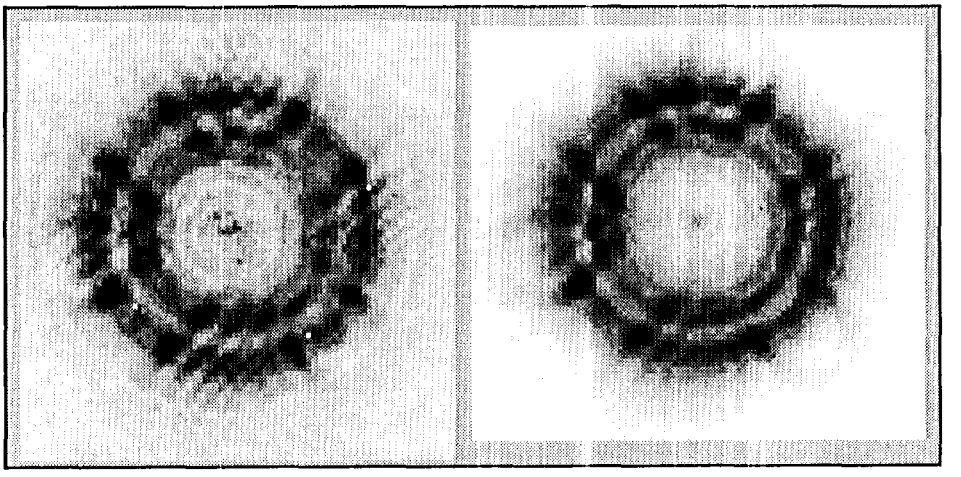

Figure 4. Data (left) and simulated (right) images from WF/PC-II, PC-1 camera (Run 2). Secondary mirror defocus=180 microns; Filter=F502N.

Table 1: Prescription retrieval preliminary results.

	"As-built"	PC1 Run 1	PC1 Run 2	WF2 Run 3	WF3 Run 4	PC1 Run 5	PC1 Run 6
OTA I'M K	-1.01390	-1.01390	-1.01390	-1.01390	-1,01390	-1.01408	–1 .01434
OTA SM K	–1 .49600	-1.49597	–1 .49597	-1.49600	-1.49579	–1.49771	–1 .50220
PC1 PM K	–0.30599	-0.30601	-0.30599			--0.?0507	-0,30386
PC1 SM K	–109.543	-109.517	-109.554			-109.621	–108.254
W1'2 PM K	-0.503155			-0.486412			
WF2 SM K	-94.4998			-92.2225			
WF3 PM K	-0.503155				-0.50323		
WF3 SM K	-94.4998				-94.4897		
Ill-focus Z11		-0.00853				-0.00927	-0.00960

The diversity in the data set is limited, as all images were taken on-axis in the cameras (not the OTA). The data does not provide displaced aberration centers, which can be useful in separating OTA and repeater figure errors. This is less true for WF/PC-II than WF/PC-I, as the optical correcting scheme places the RSM at a pupil. There is some limited separability due to the fact that changing the OTA PM conic induces astigmatism, as the beam is off-axis in the OTA, whereas changing the repeater conic

does not, as it is on axis. Separating RSM figure from the OTA I'M figure ultimately requires averaging effects across multiple cameras.We have not yet done a thorough formal error analysis of these estimates and so cannot yet comment quantitatively on the separability of the estimates,

As mentioned earlier, our main interest is in retrieving prescriptions for generating PSFS for image restoration. Most of the retrieval can be done once, using defocused images as above. Some parameters should be retrieved directly from each image to be restored, however. An example is the OTA secondary mirror focus. The HST "breathing mode" and resorption effects cause drift of the overall telescope focus over time. This is not precisely understood, but the amount of defocus can be determined by running a "tweak" retrieval using a point source from the image to be restored. Another example is the registration of dithered images, which can be determined by retrieving field angles for the same star(s) on each image separately.

Retrieval from in-focus star images is also the best approach for determining detection blurring. This phenomenon is the position-dependent probability that a photon hitting a particular pixel will register in an adjacent pixel. It is likely due to charge transfer in the CCD chip, or perhaps to scattering. We use a simple convolution model with a 3x3 kernel function, parameterized by the peak value of the kernel, to represent this effect. The blur kernel value is retrieved from in-focus data.

Figure 5 presents an example of retrieval from an in-focus image. This star appears on a set of 4 WF/PC-II, WF-3 images that were combined and restored. The basic prescription was that retrieved from the defocused data (Run 4). The in-focus image data was matched to determine the registration of the frame (pixel 235.269, 524.379), blur kernel peak value (0.79), and image defocus (6 urn). The match is quite good, as evidenced by the subtracted image, which subtracts the simulated from the data images. The restored image is also very good, with no "halo" of poorly-fit pixels surrounding; the core.

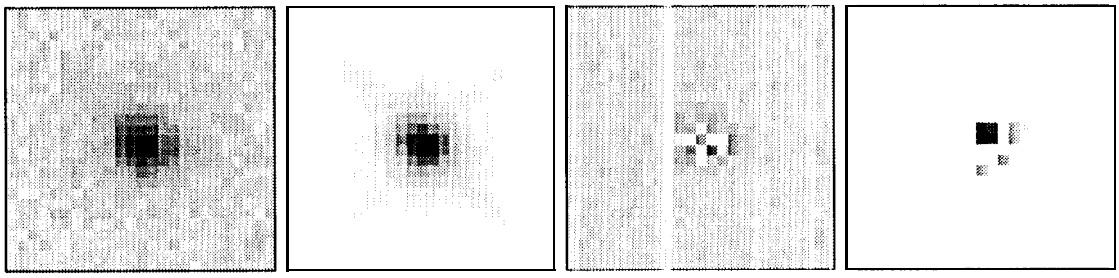

Figure 5. Data (left), simulated, subtracted and restored images from WF/PC-II, WF-3 camera (log1 O stretch). Retrieved defocus=6 microns. Retrieved blur kernel=0.79.

4. Computing Conic Constant from Spherical Aberration Data

To convert phase retrieval (*not* prescription retrieval) results to estimates of the OTA PM conic constant, the following formula has been most widely used (Furey, 1991):

$$K = KO + 1/(dZ11/dK)Z11 \qquad \text{(EQ 1)}$$

Here the coefficients are KO = -1.00223 and dZ11/dK = 35.30 in waves at 6328 Å. These coefficients were derived in the OTA only, using a limited-resolution ray-trace code. In

this section we rexamine this formula, computing new coefficients for each camera separately, using higher ray grid densities. Then we apply the new formulas to the previously reported phase retrieval results to obtain new estimates of the OTA PM conic K.

The procedure followed to generate the coefficients was as follows:

1. The OTA optical prescription was used to generate an OPD map at the exit pupil.
2. The OPD map was fitted with the 33%-obscured Zernike polynomials and the Z11 value was recorded.
3. The OTA PM K was changed to new values, and steps 1-2 were repeated for each.
4. K was plotted against the derived Zll values over the region of interest, and the linear model above was fit to the curve.

The ray sampling grid used for these coefficients was 19x1 9. Similar results were obtained using other low-density sampling grids. We have now repeated the same procedure running much larger ray grids, for each camera separately. The results are summarized in Table 2.

Table 2: Z11-to-K conversion coefficients.

Case	Camera	KO	dz11/dK	Ray Sampling	Field Point
1	OTA	-1.00223	35.30	19X19	OTA Axis (original formula)
2	OTA	-1.00223095	35.31s7	19X19	OTA Axis
3	OTA	-1.00223096	37.1200	256x256	OTA Axis
4	wfpc 1 pc6	-1.00222368	37.4123	128x128	Camera Axis (Off-axis in OTA)
5	wfpc 1 pc6	-1.00222379	36.9350	256x256	Camera Axis (Off-axis in OTA)
6	wfpc 1 pc6	-1.00227227	39.4485	256x256	OTA Axis (Off-axis in camera)
7	wfpc2 pcl	-].01354128	37.1765	256x256	Camera Axis (Off-axis in OTA)
8	wfpc2 pc 1	-1.01354409	36.5523	256x256	OTA Axis (Off-axis in camera)
9	wfpc2 wf3	-1.01335890	37.0589	256x256	Camera Axis (Off-axis in OTA)

Case 1 in Table 2 is the original formula coefficients. Case 2 repeats that case using the COMP code, showing that the results agree. Cases 5,7 and 9 provide coefficients for the WF/PC-1 PC and the WF/PC-II PC and WF cameras, respectively. Note that the KO coefficient for the WF/PC-II cameras is at the designed correction value of -1.0135. Cases 6 and 8 show that the conversion at one field angle can differ appreciably from the conversion at another. Case 4 shows sensitivity to sampling density and precise placement of the ray grid on the optics. The lesson from these cases is that these formulas should be used with non-zero error bars! The value of the error bars need not be large for a particular field / focus point in a particular camera. If a single formula is to cover all cameras and conditions, however, the error bar should be about 0.0005.

Using the new camera-specific formulas, Z11 estimates derived from phase retrieval and reported by other workers were reprocessed. The results are summarized in Table 3. The effect of the new formulas is to increase the estimated K from an averaged value of -1.0144 to an averaged value of -1.01395. This compares to estimates of -1 .01377±0.0002 and -1.01 398±0.0002 from the HARP fossil data and prescription retrieval studies,

respectively. The average of these 3 numbers is -1.01390, and all of the reprocessed phase retrieval, fossil data and prescription retrieval results lie within ±0.0002 of this number.

A word of caution is warranted. Agreement to within ±0.0002 by averaging does not provide a definitive error bar. Some sources of error were not fully characterized in the various studies. This includes the spherical aberration of the various stimuli used in testing COSTAR and WF/PC-II, which were required to meet less stringent criteria (Furey, 1994). This is significant in deriving Z11 by phase retrieval.

5. Conclusion

We have presented prescription retrieval results indicating that the official "as-built" estimates of the OTA prescription are consistent with WF/PC-11 image data. We also derived new formulas for the conversion of exit-pupil phase to OTA PM conic. These formulas were applied to estimates of the HST spherical aberration obtained by others using phase retrieval techniques. The result was an estimate of the OTA PM conic that agrees with earlier fossil data and prescription retrieval studies. Averaging results from phase retrieval, prescription retrieval and fossil data studies, the OTA PM conic is estimated to be -1 .0139t0.0002,

Improving the accuracy of the estimates of the OTA prescription parameters is important for future replacement cameras that might seek to compensate the higher-order aberrations of the OTA primary mirror (Malbet, 1995). OTA PM conic errors at the 0.0005 level could saturate the high actuator density, small stroke deformable mirrors being designed for such a mission. Further work to improve these estimates maybe desirable in light of these requirements.

Table 3: Conic constant from Z11 using new formulas.

Z11	K by new formula	K as reported	Camera	Formula (Table 2)	Reference	Notes
-0.277	-1.01404	-1.0145	FOC	3	Krist, 1995	Averages 3 wavelengths
-0,300	-1.01376	-1.0146	WF/PC-1 PC-6	5	Krist, 1995	Averages 2 wavelengths
-0.013	-1.01412	-1.0142	WF/PC-2 PC-1	7	Krist, 1995	Averages 2 wavelengths
-0.020	-1.01395	-1.0143	WF/PC-2 WF-2	9	Krist, 1995	Averages 2 wavelengths
-0.024	-1.01400	-1.0144	WF/PC-2 WF-3	9	Krist, 1995	Averages 2 wavelengths
-0.023	*-1.01394*	*-1.0143*	WF/PC-2 WF-4	9	Krist, 1995	Averages 2 wavelengths
-0,290	-1.01369	Not given	WF/PC-1 PC-6	5	Roddier, 1993	
-0.299	-1.01408	1-1.0144	WF/PC-1	5	Fienup, 1993-	

6. Acknowledgement

Research described in this paper was carried out at the Jet Propulsion Laboratory, California institute of Technology, under contract with the National Aeronautics and Space Administration.

7. References

1. A. Boden, D. Redding, J. Mo, R. Hanisch and R. White, "Comparative Results with Massively Parallel Spatially-Variant Maximum Liklihood Image Restoration," Bulletin of the American Astronomical Society, V. 27, No. 2, pp. 924-929 (1995).
2. *OTA Handbook Version 1.0,* C. Burrows, (Ed.), STScI Publication (May 1990).
3. *Wide Field and Planetary Camera 2 Instrument Handbook* , C. Burrows, (Ed.), STScI Publication (June 1995).
4. J. Fienup, J. Marron, T. Schulz and J. Seldin, "Hubble Space Telescope Characterized by Using Phase Retrieval Algorithms," Applied Optics, V. 32, No. 10 (April 1993).
5. L. Furey, "Derivation of the FIST Primary Mirror Conic Constant from Fossil Data," HDOS Report (July 1991).
6. L. Furey, T. Dubos, D. Hansen and J. Samuel s-Schwartz, "Hubble Space Telescope Primary Mirror Characterization by Measurement of the Reflective Null Corrector," Applied Optics, V. 32, No. 10 (April 1993).
7. L. Furey, "Post-FSM Optical Prescription Status Report," H DOS Memo A16-ST-0331 (May 1994).
8. J. Krist and C. Burrows, "Phase Retrieval Analysis of Pre- and Post-Repair Hubble Space Telescope Images," ST SCI Preprint No. 901 (1995). To appear in Applied Optics.
9. F. Malbet, J. Yu and M. Shao, "High-Dynamic-Range Imaging Using a Deformable Mirror for Space Chronography," PASP, Vol. 107, No. 710 (1995).
10. D. Moore et al, HIORP Final Report (1991).
11. D. Redding, M. Lee and S. Sirlin, "Improved Prescription Retrieval and Modeling Code," in *The Restoration of HST images and Spectra II,* R. Hanisch and R. White, eds. (1 994).
12. D. Red ding, L. Needels, K. Wallace and J. Yu, *Controlled Optics Modelling Package User Manual,* JPL Document D-9816 (June 1992).
13. D. Redding, P. Dumont and J. Yu, "Hubble Space Telescope Prescription Retrieval," Applied Optics, V. 32, No. 10 (April 1993).
14. C. Roddier and F. Roddier, "Combined Approach to the Hubble Space Telescope Wavefront Distortion Analysis," Applied Optics, V. 32, No. 16 (June 1993).
15. M. Shao, M. Colavita, R. Dekany, P. Dumont, B. 1 Iines, M. Levine, D. Redding, S. Brewer and A. Decou, "Image inversion Analysis of Hubble Space Telescope Optics Using a Non-linear Least-Squares Algorithm," JPL Report (1991).

Optical Prescription of the El ST

David Redding, Sam Sirlin, Andy Boden
Jet Propulsion Laboratory, California Institute of Technology
Jinger Mo, Bob Hanisch
Space Telescope Science institute
Laurie Furey
Optical Archeology, Inc.
July 18,1995

Introduction

The optical prescription of the Hubble Space Telescope - in particular the conic constant of the primary mirror - received a lot of attention following discovery of the spherical aberration of the primary mirror. The concern then was to design appropriate corrective optics for WF/PC-II and COSTAR. This concern remains today, though at a different level, for builders of future instruments, especially of instruments that might seek to compensate actively or passively for primary mirror (PM) aberrations on a finer spatial scale (Malbet, 1995).

Under the Hubble Aberration Recovery Program (HARP), several groups independently determined estimates of the PM conic (Moore, 1991) Complete agreement among the groups was not achieved. Those who examined the fabrication and test hardware (the "fossil data" study) derived a number for the PM conic of -1 .01377±0.0003 (Furey, 1993). Several more groups who employed phase retrieval techniques derived numbers ranging from -1.0137 to -1.0150 (eg, Fienup, 1993; Roddier, 1993; Shao, 1991). The official estimate used to build COSTAR (-1.0139) averaged results from several studies, but did not resolve the differences. These differences were emphasized again recently, with publication of phase retrieval results from WF/PC-II data indicating a value for the primary mirror conic constant of -1.0144 (Krist, 1995).

Also as part of the HARP effort, a direct prescription retrieval technique was developed and applied (Redding, 1993). Like phase retrieval, prescription retrieval is an "image inversion" parameter estimation approach, where a computer model of the optical system is used to generate simulated images that are matched iteratively with data images. The HARP prescription retrieval results agreed with the fossil data studies, with an estimate of -1 .0139W0.0002.

Prescription retrieval differs from phase retrieval in the parameterization of the image-inversion problem. It uses a hybrid ray-trace and diffraction modeling code to solve *directly* for the conic constant and other prescription parameters. By contrast, phase retrieval techniques solve for intermediate parameters wavefront phase parameters, usually Zernike polynomials. The effect of the conic constant error appears as spherical aberration, or the 11th Zernike polynomial coefficient ("Z11") in the 330/O-obscured form used by most HST investigators. In a crucial step, the conic constant is then estimated from Z11 using a simple formula derived using ray-trace techniques (Furey, 1991).

in this paper, we report new results using prescription retrieval to estimate the PM conic from WF/PC-II focus run images. These preliminary results agree with the HARP fossil data and prescription retrieval results. They disagree with reported estimates of PM conic derived from phase retrieval results using the old formula.

To resolve these differences, we reexamine the formula used to compute conic constant from Z11. Using higher ray densities than were available originally, and computing formulas for each camera separately, new formulas are derived. These formulas are used to reprocess the spherical aberration results reported by the phase retrieval studies. The resulting estimates of conic constant are in agreement with the earlier official estimate.

Combining all results (reprocessed phase retrieval, fossil data and prescription retrieval), the primary mirror conic constant is estimated to be -1 .0140±0.0003.

The HST prescription is also of interest for image restoration purposes. We use prescription-based PSF generation codes to support spatially-variant-PSF image restoration (Red ding, 1994; Boden, 1995). Prescription retrieval is used to obtain the accurate prescription data needed to generate representative PSFs.

Prescription Retrieval

The HST Optical Telescope Assembly (OTA) consists of a primary and a secondary mirror, plus supports and baffles, forming a Ritchey-Chretien telescope (Burrows, 1990) (Fig.). The WF/PC imaging camera optics follow the OTA optics, beginning with a pickoff mirror (POM) at the center of the OTA field of view (Burrows, 1995). Then comes the filter wheel and a pyramid mirror, which splits the field of view into 4 separate cameras. Within each camera there is a fold mirror followed by the WF/PC repeater optics, These consist of a repeater primary (RPM), secondary mirror (RSM), and CCD detector assembled together in a barrel structure. Field curvature is corrected by a plano-concave field flattener lens mounted immediately in front of the detector.

in WF/PC-II, the pupil is reimaged at the RSM, which is figured to compensate for the spherical aberration of the OTA primary. The WF/PC-II design was frozen before the HARP results were finalized, however. The best estimate of K at the time the RSM design was frozen was -1.0135, **so** this is the value that the compensation was designed to null. Later results showed the primary to be slight] y more aberrated (K = -1 .0139). The result is that the WF /PC-11 compensation leaves a small residual spherical aberration, which is seen in the data.

The precise footprint of the beam on the WF/PC-II RSM can be adjusted cm-orbit by tilting the pick-off mirror and, in PC-1, WF-3 and WI '-4, by tilting the camera fold mirrors. Errors in placing the beam on the RSM result in coma in the image.

Focus is adjusted by axial translation of the OTA secondary. The OTA secondary can also be recentered to recollimate the telescope. Small misalignments incurred in fabrication are to be expected in the repeater barrel position and angle, plus all individual optics,

Obscurations affecting the image are incurred at the OTA secondary support spiders and baffles, and at the OTA primary, where 3 small support pads are visible at the edges of the aperture. The entrance aperture is placed about 100 mm ??? ahead of the primary mirror, defining the system stop. There is field-angle dependent vignetting at the filters and at the RSM. The location in the pupil of the RSM obscurations is also strongly dependent on field angle. The amount of light passed by the HST and WF/PC-II system varies by over 20% ??? over the full WF field. These effects are detailed in (Holtzman, 1995).

In addition to the shearing obscuration effects, there are induced aberrations and distortion that occur with changes in field angle. Small amounts of coma and astigmatism are seen at the edges of the field (Ref. ???). The distortion effects are reviewed in **(Ref. Vaughan).**

All of these systematic effects on the HST PSF can be accurately predicted from the optical prescription using a combination of ray-trace and physical optics techniques. Here "optical prescription" means the data defining the orientation, location, figure and index of each optical element. Prescription-based ray-trace codes can accurately determine the wavefront phase and obscuration patterns induced by changing field angles, changing focus or decenter of the secondary, or by misalignment of any of the other optics in the beam train. This is how optical systems are designed, after all.

Fourier optics diffraction beam propagators can then be used to convert ray-based phase information into a TE comple-amplitude matrix describing the diffracted beam (Ref. Reading???). This can be done at multiple points in the beam train, if desired, though it is usually sufficient to use only a single diffraction propagation, from the exit pupil to the detector. The detected intensity is the modulus squared of the field at the detector, resampled into the CCD pixel geometry. Detection effects, such as charge-transfer blurring, motional blurring and noise can then be added.

This approach to modeling optical instruments is realized in a general-purpose optical modeling code called COMP (Ref. COMP). COMP uses the optical prescription to define the image-forming beam train. It uses a full general ray-trace engine to trace a bundle of rays defined at entrance pupil past each optical, vignetting or obscuring surface. The phases computed by the ray-trace drive Fourier beam propagators, which compute the diffracted beam at the detector. For most results reported here, only 1 diffracting surface was used, located at the WF/PC exit pupil.

The COMP model provides means to capture the systematic behavior of the images – provided accurate prescription data is used. In general, the design prescription, or even a prescription incorporating results of ground testing will not capture the full performance of the instrument. Means to improve estimates of prescription parameters beyond pre-launch values are provided by prescription retrieval.

Prescription retrieval is an iterative parameter optimization process (Fig. 2), taking the optical design prescription as a starting point, generating images at particular field and focus settings, and matching these images to data images taken under the same conditions (Refs). The match is improved by varying selected prescription parameters.

Some parameters vary with each image in a set, such as field angle, flux, background, and focus setting. Other parameters are common to a set of images, such as OTA and WF/PC mirror figure parameters, OTA higher-order figure errors, WF/PC barrel alignments, and pickoff mirror and fold mirror tilts.

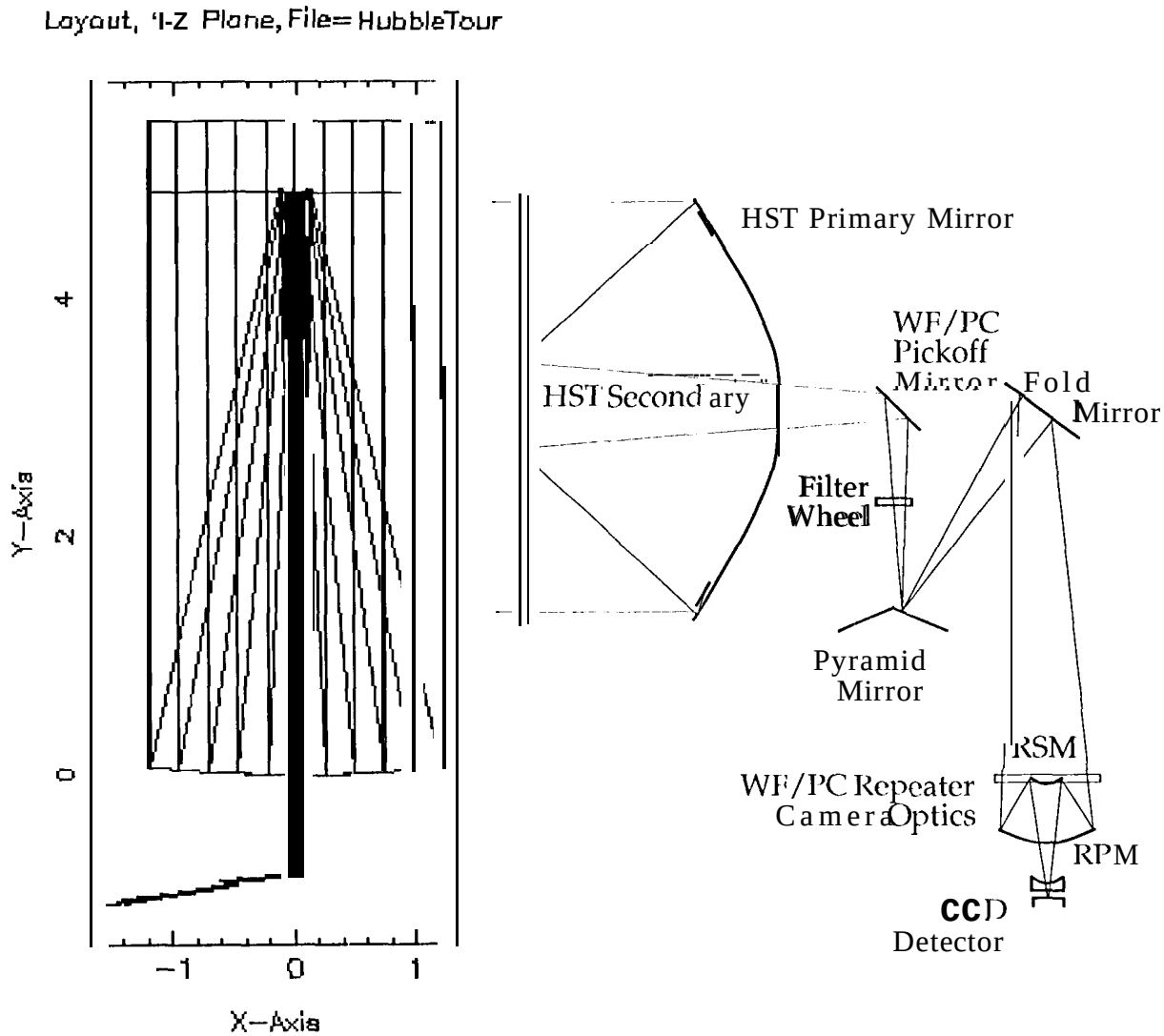

Figure 1. Ray-trace of the HST and WF/PC-I

To get good results for most parameters, a good set of diagnostic images is needed. This should include images taken at multiple focus positions, at multiple field points, and in multiple cameras. Defocusing spreads out the images across many pixels, exposing the signature of the aberrations, such as the spherical aberration rings, and improving the ability to resolve these features. Data taken from both sides of focus resolves ambiguities between asymmetric surface figure aberrations. Defocusing also brings out the obscuration patterns, which help identify alignments. Field diversity shears the effects induced at different surfaces. This was useful in WF/PC-I retrievals, as it separated the aberration centers of the OTA optics from the aberration centers of the repeater cameras: the OTA aberrations remain centered while the camera aberrations shift center with field

angle, improving the separability of these contributors to the overall HST spherical aberration.

Prescription retrieval is a better approach than phase retrieval for determining the prescription of an instrument, because it directly solves for the parameters of interest in a model that accurately represents their effect on the data. On the other hand, phase retrieval can be very effective in matching particular images, e.g. (Roddier, 1993). Zernike polynomials provide a less-constrained, nearly orthonormal phase parameter set compared to prescription parameters. Non-parametric phase retrieval has the further advantage of a very large number of degrees of freedom for matching data. The problems with phase retrieval have to do with converting the phase information to prescription information, and in extrapolating fits at one point in the field to another. Generalizing the good match at one point to predict the PSF at another point using a conventional physical optics model requires separately identifying and fitting models to all of the systematic variations that occur with changes in field angle. This includes shearing obscurations, shearing figure errors, and varying aberration terms with field angle. Prescription-based models provide a better basis for predicting these systematic effects.

Either approach can be carried too far, by overfitting the data at high spatial frequencies, so that effects such as scattered light and detection blurring can be incorrectly attributed to optical aberrations. The likelihood of this can be reduced by avoiding scattered or stray light conditions in the data, by including detection blurring in the model, and by using a sufficiently large and diverse data set.

Figure 2. Sketch of prescription retrieval process.

WF/PC-II Prescription Retrieval Preliminary Results

This section reports preliminary results of prescription retrieval using defocused WF/PC-11 images taken under a proposal by C. Burrows. These images were taken on-axis, at 4 focus settings (±360 urn and ±180 urn defocus). They were taken in all 4 cameras, using 3 narrow-band filters. Two images were taken for each setting. Cosmic-ray and saturated pixel identification was performed to generate masks for each image. Most results were

run with combined images (the 2 images were added), though some were run with single images.

The objective of this first round of retrievals was to determine if the defocused images are consistent with previous estimates of the prescription parameters. The starting prescription was taken to be the WF/PC-II project official "as-built" Code V'[M] prescription. Image-specific parameters varied were field angle, flux, background, and focus setting. System parameters, assumed the same in each image, were the conic constants of the OTA primary and secondary, the conic constants of the repeater camera primary and secondary, WF/PC barrel alignments, and pickoff mirror and fold mirror tilts. In addition, 2 of the runs included Zernike figure errors on the primary mirror. No detection blurring was included in these retrievals.

The individual images were fit fairly well at lower spatial frequencies. The main features for determining the conic constants, namely the bright spherical aberration rings, appear at the same positions. Other features were not matched as well, and we expect that including higher spatial-frequency figure errors and detector blurring and will improve the overall match. Figure 3 shows images from PC1 Run 2, comparing simulated and data images for OTA secondary mirror defocus= 360 um. Figure 4 compares simulated and data images for defocus = 180 um. .

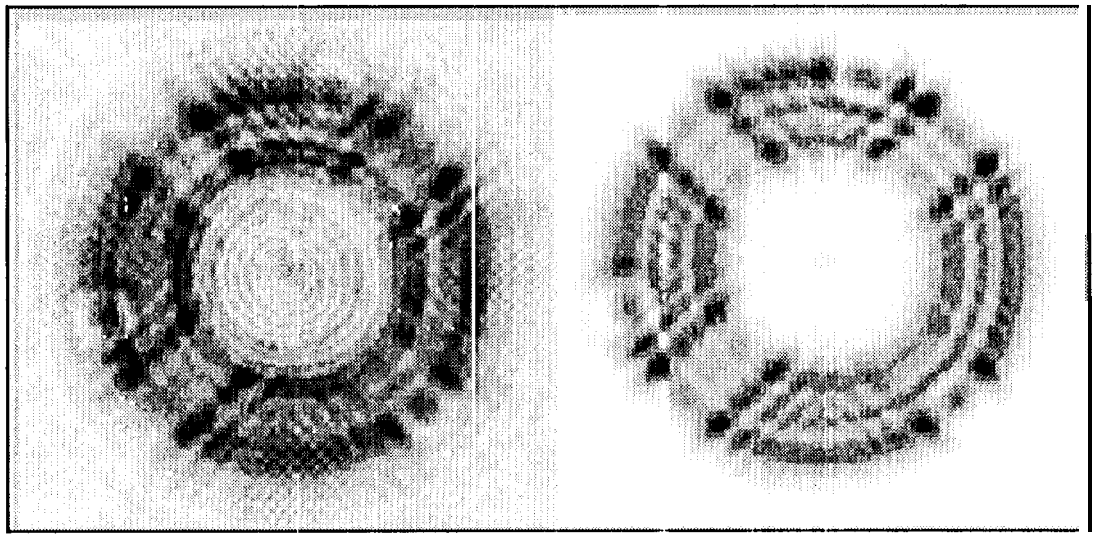

Figure 3. Data (left) and simulated (right) images from WF/PC-II, PC-1 camera (Run 2). **Secondary mirror defocus=360 microns; Filter=F502N.**

The results for mirror conic constants are summarized in Table 1.The initial parameter values for the first 4 runs were set to the "as built" official estimates. All conies were allowed to vary, together with other image and system parameters. The Z11 numbers were fit to OI?D maps generated using the retrieved prescriptions. The results show very little change in the estimates of the OTA conic constant parameters. The PC-1 repeater conic constant estimates also change very little. This is consistent with test results that show only a very small amount of spherical aberration in the PC-1 repeater camera (Krist, 1995). The estimates of the WF-2 repeater conies change more significantly; those for WF-3 change very little.

To test the hypothesis that the OTA PM conic is actually less than -1.0139, and to test the separability of the conic parameters, initial values for the last 2 cases were set at lower values (-1 .0141 and -1.0144, respectively). The results show that the increased spherical aberration from the PM is countered by changes in the estimated conies for the other cameras, so that the net spherical aberration remains about the same. The Z11 computed from the retrieved prescriptions agree with Z11 values derived from WF/PC-II phase retrieval (projected to in-focus conditions), to the accuracy of the claimed error bars (Krist, 1995). The results also show that this data dots not provide sufficient diversity to conclusively separate the effects induced at the various surfaces. This is indicated by the fact that the estimates from different starting points did not converge to the same numbers. in this case, the most likely results are those which require the least change in the "as built" a priori estimates (which are derived from test data): runs 1 to 4.

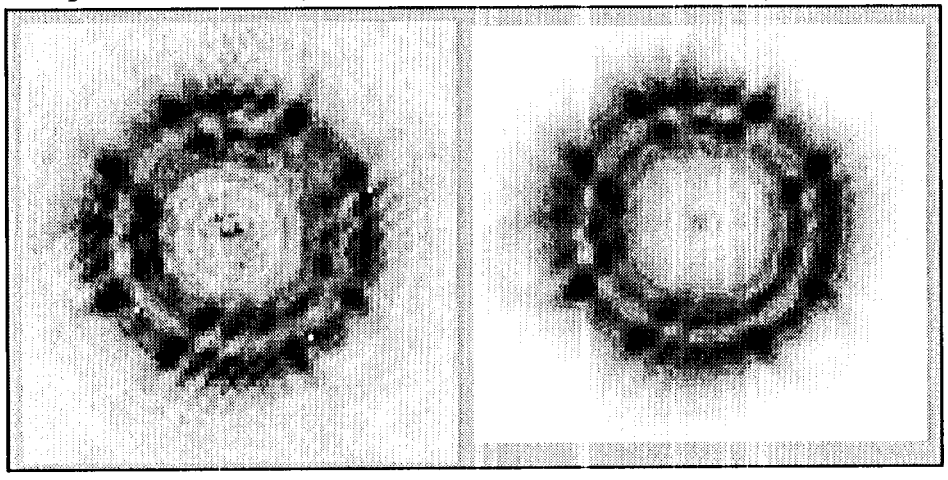

Figure 4. Data (left) and simulated (right) images **from WF/PC-I 1, PC-1 camera (Run 2). Secondary mirror defocus= 180 microns; Filter=F502N.**

'1'able 1: WF/PC-II prescription retrieval results. All runs used filter F502N. Runs 2 and 4 included 36 OTA PM figure error Zernike polynomials in addition to image, conic and alignment parameters.

	"As-built"	PC1 Run 1	PC1 Run 2	WF2 Run 3	WF3 Run 4	PC1 Run 5	PC1 Run 6
OTA PM K	-1.01390	-1.01390	-1.01390	-1.01390	-1.01390	-1.01408	-1.01434
OTA SM K	–1 .49600	–1 .49597	–1 .49597	–1 .49600	–1 .49579	--1.49771	-1.50220
PC 1 PM K	-0.30599	–0.3060 1	-0.30599			--0.30507	-0.30386
PC 1 SM K	– 109.543	-109.517	-109.554			--109.621	-108.254
WF2 PM K	-0.503155			-~1486412			
WF2 SM K	-94.4998			--92.2225			
WF3 PM K	-0.503155				-0.50323		
WF3 SM K	-94.4998				-94.4897		
Ill-focus Z11	-0.00841	-0.00853				-0.00927	-0.00960

These results indicate that the "as-built" estimates for the conic constants of the HST and WF/PC-II optics are consistent with the data being received from the telescope. These results are not conclusive, however. The diversity in the data set is limited, as all images were taken on-axis in the cameras (not the OTA). The data does not provide displaced

aberration centers, which can be useful in separating OTA and repeater figure errors. This is less true in WF/PC-II than in WF/PC-I data, as the optical correcting scheme places the RSM at a pupil. There is some limited separability due to the fact that changing the OTA PM conic induces astigmatism, as the beam is off-axis in the OTA, whereas changing the repeater conic does not, as it is on axis. Separating RSM figure from the OA PM figure ultimately requires averaging effects across multiple cameras. We have not yet done a thorough formal error analysis of these estimates and so cannot yet comment quantitatively on the separability y of the estimates.

As mentioned earlier, our main interest is in retrieving prescriptions that we can use for generating PSFS for image restoration. Most of the retrieval can be done once, using defocused images as above. Some parameters should be retrieved directly from the image to be restored, however. An example is the OTA secondary mirror focus. The HST "breathing mode" and resorption effects cause drift of the overall telescope focus over time. This is not precisely understood, but the amount of defocus can be determined by running a "tweak" retrieval using a point source from the image to be restored. Another example is the registration of dithered images, which can be determined by retrieving field angles for the same star(s) on each image separately.

Another parameter that is best retrieved from in-focus star images is the detection blurring. This phenomenon is likely due to charge transfer in the CCD chip, or perhaps to scattering, and presents a position-dependent probability that a photon hitting a particular pixel will register in an adjacent pixel (CCD Ref.). We use a simple convolution model with a 3x3 kernel function, parameterized by the peak value of the kernel, to represent this effect. The blur kernel value can be retrieved easily from in-focus data.

Figure 5 presents an example of retrieval from an in-focus image. This star appears on a set of 4 WF/PC-II, WF-3 images that were combined and restored (Ref. HH47). The image data was matched to determine the relative registration of each frame, the blur kernel peak value (0.79), and the image defocus (6 um).

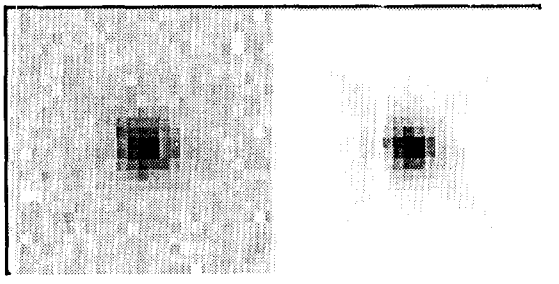

Figure 5. Data (left) and simulated images from WF/PC-II, WF-3 camera (log10 stretch). Retrieved "breathing" defocus=6 microns. Retrieved detection blurring kernel=0.79.

Computing Conic Constant from Spherical Aberration Data

The prescription retrieval results presented here indicate that the official "as-built" estimate of the conic constants of the OTA optics is consistent with the images being received from space. Why, then, do some workers using phase retrieval report higher

numbers? We reexamine the formula relating spherical aberration and conic constant in this section.

For HARP studies, main formula used was . . . The coefficients of this formula were" "" estimated using ray trace anal. An opdes code using the HST OTA presc was used to generate OTA exit pupil phase maps for a particular val of K. 33% obscured Zerns were fit to the phase map. The sph ab component (Z11) was determined. I'recess repeated for a range of vals of K. Linear regression then used to fit this data and determine values of coefs. The form is inverted to obtain eq ???

The op des code used originally had limited res. Data was generated using 19x19 square grid, and checked using a polar grid of similar density.

We have now gone back and repeated this work using higher resolution code. We also reran the process for each camera separately, and looked at off-axis points.

Table 2: New Z11-to-conic constant conversion formula coefficients.

Case	Camera	K0	dz11/dK	Ray Sampling	Field Point
1	OTA	-1.00223	35.30	19x19	OTA Axis
2	OTA	-1.00223025	35.3157	19X19	OTA Axis
3	OTA	-1.00223096	37.1200	256x256	OTA Axis
4	wfpc 1 pc5	-1.00222368	37.4123	128x128	Camera Axis (Off-axis in OTA)
5	wfpc 1 pc5	-1.00222379	36.9350	256x256	Camera Axis (Off-axis in OTA)
6	wfpc 1 pc5	-1.00227227	39.4485	256x256	OTA Axis (Off-axis in camera)
7	wfpc2 pc1	-1.01354128	37.1765	256x256	Camera Axis (Off-axis in OTA)
8	wfpc2 pc 1	-1.01354409	36.5523	256x256	OTA Axis (Off-axis in camera)
9	wfpc2 wf3	-1.01335890	37.0589	256x256	Camera Axis (Off-axis in OTA)

'J'able 3: New conic constant estimates from phase retrieval Z11

Z11	K by new formula	K as reported	Camera	Reference	Notes
-0.277	-1.01404	-1.0145	"Foe	Krist, 1995	Averages 3 wavelengths
-0.300	-1.01376	-1.0146	WF/PC-1 PC-6	Krist, 1995	Averages 2 wavelengths
-0.013	-1.01412	-1.0142	WF/PC-2 PC-1	Krist, 1995	Averages 2 wavelengths
-0.020	-1.01395	-1.0143	WF/PC-2 WF-2	Krist, 1995	Averages 2 wavelengths
-0.024	-1.01400	-1.0144	WF/PC-2 WF-3	Krist, 1995	Averages 2 wavelengths
-0.023	-1.01394	-1.0143	WF/PC-2 WF-4	Krist, 1995	Averages 2 wavelengths
-0.290	-1.01369	Not given	WF/PC-1 PC-6	Roddier, 1993	
-0.299	-1.01408	-1.0144	WF/PC-1	Fienup, 1993	

'J'able *4:* HST conic constant summary.

K	Explanation
-1.01395	Average of recomputed phase retrieval results
-1.01377	Fossil data
-1.01398	Prescription retrieval

Discussion

What level of accuracy reqd for follow-on inst? Ref 1 uses hi-dens DM to comp I'M zones and create a "dark hole" of low scattered light for direct det of planets orb nearby stars. The DM specs call for p2p stroke of 0.1 um. The main objective for a presc ret then is probably to determine K accurately enough that errors not produce resids that sat the DM stroke.

Conclusion

Pres PR res from WF/PC-I 1 that show official as-built estimates of OTA presc are consistent with the data, Not consist with conclusions of wotrkers who used phase retrieval, however. To reconcile other worker's phase retrieval results, re-examined form for conv between conic and phase parameters. Computed new form in the particular cams, and at higher ray dens. Reprocessed phase nums with new form to get new est of K from reported Z11. New results agree with official est, PR and fossil fdata results, suggesting that K is .,.

Nonetheless, these results indicate that the official numbers for the OTA conic constants are consistent with the data, and do not provide grounds for changing the estimate of the OTA conic constants.

Acknowledgement

Research described in this paper was carried out at the Jet l'repulsion Laboratory, California institute of Technology, under contract with the National Aeronautics and Space Administration.

References

1. F. Malbet, J. Yu and M. Shao, "High-Dynamic-Range Imaging Using a Deformable Mirror for Space Chronography," PASP, Vol. 107, No. 71O(1995).
2. D. Moore et al, HIORP Final Report (1991).
3. L,. Furey, T. Dubos, D. Hansen and J. Samuels-Schwartz, "Hubble Space Telescope Primary Mirror Characterization by Measurement of the Reflective Null Corrector," Applied Optics, V. 32, No.10(1993).
4. J. Fienup, J. Marron, T. Schulz, J. Seldin, "1 Iubble Space Telescope Characterized by Using Phase Retrieval Algorithms," Applied Optics, V. 32, No. 10 (1993).
5. Roddier and Roddier

6. M. Shao, M. Colavita, R. Dekany, I'. Dumont, B. Hines, M. 1 evine, D. Redding, S. Brewer and A, Decou, "image Inversion Analysis of Hubble Space Telescope Optics Using a Non-Linear Least-Squares Algorithm," JP'L Report (1991).

7. J. Krist and C. Burrows, "Phase Retrieval Analysis of Pre- and Post-Repair Hubble Space Telescope Images," ST SCI Preprint No. 901 (1995). To appear in Applied Optics.

8. D. Red ding, P. Dumont and J. Yu, "Hubble Space Telescope Prescription Retrieval," Applied Optics, V. 32, No. 10 (1993).

9. L. Furey, paper on formula.

10. D. Redding, M. Lee and S. Sirlin, "Improved Prescription Retrieval and Modeling Code," in The Restoration of HST Images and Spectra 11, R. Hanisch and R. White, eds. **(J994).**

11. A. Boden, D. Redding, J. Mo, R. Hanisch and R. White, "Comparative Results with Massively Parallel Spatially-Variant Maximum Liklihood Image Restoration," Bulletin of the American Astronomical Society, V. 27, No. 2 (1995). In press.

12. "Jets from Young Stars,''...

13. *OTA Handbook Version 1.0, C.* Burrows, (Ed.), STScI Publication (May 1990).

14. *Wide Field and Planetary Camera 2 Instrument Handbook, C.* Burrows, (Ed.), STScI Publication (June 1995).

15. Holtzman.

From Laurie's materials

1. Paragraph on costar results

2. Numbers from formula runs

3.

To be done for Applied Optics paper:

1. More thorough PR

- No flat field
- Single images

2. Formal error: test for separability

3.